Silicon Microstructures

DOI: 10.1002/anie.200907271

Double-Helical Silicon Microtubes**

Haruhiko Morito and Hisanori Yamane*

The various helices that occur in nature, for example, conch shells, vines of plants, and the DNA in our somatic cells, are fascinating with their infinite helical geometry. Helical structures are also artificially created in art and industry. Carbon nanotubes are the most famous materials with helical structures, on which the electronic behavior of the nanotubes depends.[1–3] Helical coils of carbon and silicon carbide (SiC) as well as helical belts of zinc oxide (ZnO) have also been synthesized and have attracted much attention to the potential of helical shapes.[4–6] Silicon bulk crystals and thin films are widely used for electric devices and solar batteries. Whiskers, nanowires, and nanotubes of Si have also been fabricated.[7–11] However, helical structures of silicon have not been reported. In the present study, we succeeded in synthesizing double-helical microtubes of silicon by a new method in which a Zintl compound NaSi was used as the starting material.[12]

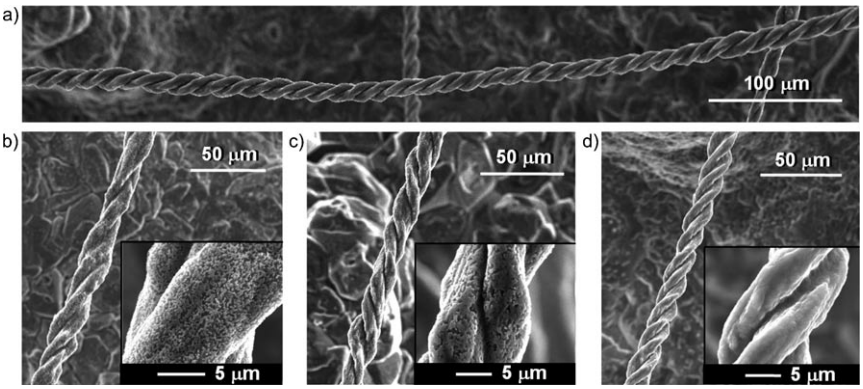

Figure 1. Scanning electron micrographs of the double-helical Si microtubes prepared by heating the Zintl compound NaSi. a) A long view of a left-handed double-helical Si microtube. Enlarged views showing the surface texture of b) a left-handed and c) a right-handed double-helical tube with a nanogranular surface structure and d) a left-handed double-helical tube with a smooth surface.

Details of the synthetic procedure are described in the Experimental Section. A disk of compacted NaSi powder was heated from room temperature to 800 °C for 1 h in a temperature-gradient reactor. This temperature was maintained for 12 h, and Na was evaporated from the NaSi disk. After the heating, a disk of polycrystalline Si was obtained. A large number of microtubes were obtained on the disk surface (Figure S1 in the Supporting Information). Wires of about 10–50 μm in diameter grew from the top of protuberances of the surface. The lengths of the wires ranged from about several hundred micrometers to 2.5 mm. Figure 1 shows SEM images of the wires observed on the sample. Most wires had double helical structures with various surface morphologies such porous, bumpy, or smooth at nanometer scale (Figure 1 b–d). Both right- and left-handed double helices were observed (Figure 1 b,c).

An X-ray diffraction photograph of a double helical wire was taken with a single-crystal X-ray diffractometer equipped with an imaging plate. A Debye–Scherrer ring pattern in which each ring was indexed with the cell parameter of Si (cubic $Fd\bar{3}m$, $a = 5.431$ Å) was observed (Figure 2 a).[13] This pattern clearly indicates that the wire consists of polycrystalline silicon.

The fracture cross sections of the protuberance and the helical wire are shown in Figure 2 b,c. Wrinkles were seen on the protuberance, and the grains on the surface were as fine as on the wires. Two or three double-helical wires sometimes grew from the top of a protuberance. The cross section of the wires was flat, and the fracture surface was smooth. There was a flattened hole through the protuberance which continued to the inside of the double helical wire (Figure 2 b,c and Figure S2 in the Supporting Information). Every sample without exception had a hole. The tip of the double-helical wire was sharp and closed (Figure 2 d). These observations indicate that the double-helical wires obtained in the present study were closed-ended microtubes.

Figure 3 a shows an optical microscopy photograph of a thin section of a double-helical microtube for TEM observation. The cutting plane of the section was off the tube growth direction. Two pores a few micrometers large were observed in the section. In a bright-field image of the TEM photograph taken for the area indicated by a dotted line in Figure 3 a, an intricate texture of crystal domains was observed (Figure 3 b). In addition, many angular pores less than 10 nm large were

[*] Dr. H. Morito, Prof. Dr. H. Yamane
Institute of Multidisciplinary Research for Advanced Materials
Tohoku University
2-1-1 Katahira, Aoba-ku, Sendai 980-8577 (Japan)
Fax: (+81) 22-217-5813
E-mail: morito@tagen.tohoku.ac.jp

[**] We thank S. Ito for preparing a thin section of the sample and for TEM observations. We are also grateful to Dr. Y. Hayashi and Prof. R. Kainuma for their help with the digital optical microscope (KEYENCE, VHX-1000) and the scanning electron microscope (SEM, KEYENCE, VE-9800). This work was supported in part by a Grant-in-Aid for Young Scientists (Start-up) from the Ministry of Education, Culture, Sports, Science and Technology (No. 20860016).

Supporting information for this article is available on the WWW under http://dx.doi.org/10.1002/anie.200907271.

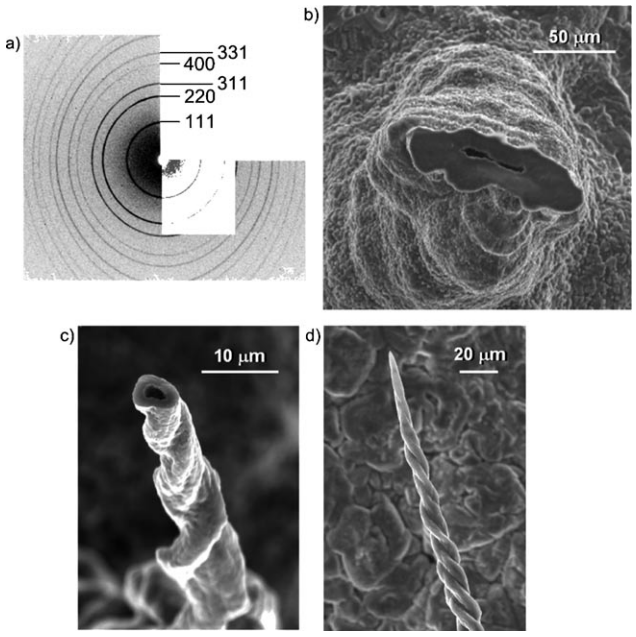

Figure 2. a) X-ray Debye–Scherrer ring pattern of a double-helical microtube. Scanning electron micrographs of the fracture cross sections of b) a protuberance on the Si disk and c) a double-helical Si microtube; and d) the tip of the microtube.

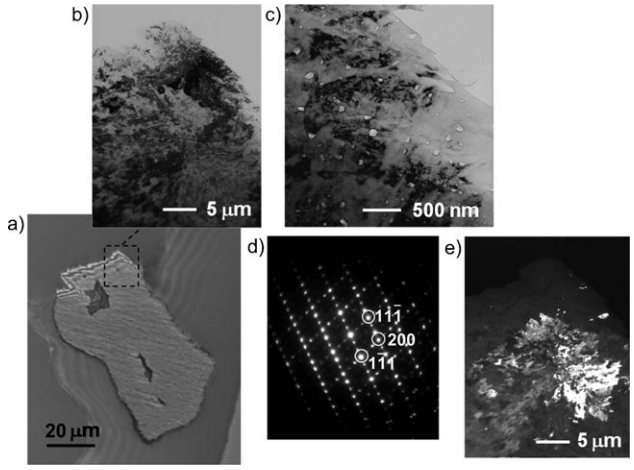

Figure 3. a) Optical micrograph of a thin section of the double-helical Si microtube. Bright-field transmission electron micrographs taken under b) lower and c) higher magnification for the area shown in the picture with a dotted line in (a). d) A selected area electron diffraction pattern, and e) a dark-field transmission electron micrograph taken for the 11$\bar{1}$ diffraction peak.

clearly observed under higher magnification throughout the sample (Figure 3c). Figure 3d shows an electron diffraction (ED) pattern from a selected area of the specimen shown in Figure 3b. Although the XRD pattern of the sample exhibited a ring pattern, a spot pattern with streaks and extra spots, which could not be explained by the structure of Si (cubic $Fd\bar{3}m$), was observed in the ED pattern. Very similar odd ED patterns with extra spots and streaks have previously been observed in Si nanowires and thin films.[14] Recently, Cayron et al. investigated such odd ED patterns by TEM and high-resolution TEM observation and by simulation.[14] They concluded that such patterns result from both microtwinning and nanotwinning of Si. The dark-field image taken for 11$\bar{1}$ ED shown in Figure 3d also indicated that the area of the 11$\bar{1}$ diffraction plane was distributed widely in the specimen without specific outlines of grains. It became clear that the inside of the helical tube wall was not composed of granular Si grains. The microtwinning and nanotwinning textures suggest that the helical Si wires directly crystallized from the liquid phase.

There are various methods for the fabrication of microwires, nanowires, and nanotubes.[15] The method using the vapor–liquid–solid (VLS) mechanism is a representative one for the growth of Si wires and whiskers.[7] In this process, the target element of Si supplied from a vapor phase dissolves into a liquid droplet of a catalyst metal, for example, Au, followed by nucleation and growth of single crystalline rods and wires. The solution–liquid–solution (SLS) method and supercritical fluid–liquid–solid (SFLS) method are other synthetic methods.[8,9] Solutions and supercritical fluid are used to supply Si to the liquid droplet of a catalyst metal. Au or Bi is used for a catalytic metal solvent in these methods. The catalyst metals are usually crystallized on the top of the wire and rods formed in the VLS, SLS, and SFLS processes. The tips of the double-helical microtubes obtained by the present study were sharp, as shown in Figure 2d, and no element other than Si was detected at the tips of the tubes by energy-dispersive X-ray (EDX) analysis, thus indicating that helical tubes were grown not by VLS, SLS, or SFLS mechanisms but by another different mechanism.

In a previous study, a nanowire of ZnS was used as a template to fabricate Si nanotubes. Si was deposited on the surface of the nanowire, and the template was removed later.[10] An Al_2O_3 tube was used as a mold in another method.[11] The synthesis of Si microtubes has also been carried out by evaporation of SiO_2 without templates.[16] The mechanism of the double-helical microtube formation is probably different from the previously proposed mechanisms for Si microtube fabrication.

Recently, we measured the melting point of NaSi at 798 °C and the eutectic point of NaSi and Si at 750 °C, and proposed a NaSi binary phase diagram.[17] In that study, NaSi with a droplet shape was crystallized by heating at 800 °C and by cooling from this temperature. In the present study, the NaSi disks were heated in the reactor with a temperature gradient. Evaporation of Na from the disk and condensation of Na in a cooler part of the reactor occurred while the disk was heating up to the eutectic point. The formation of Si clathrate compounds (Na_8Si_{46} and Na_xSi_{136} ($x \leq 24$)) by heating NaSi at above 360 °C under a reduced pressure has been investigated.[18–21] Na_8Si_{46} and Na_8Si_{136} decompose into Si at over 520 °C and 606 °C, respectively.[20,21] In the present study, Si clathrates were not detected in the disks and tubes by XRD or ED. The Si crystals may have been formed by Na evaporation from NaSi without formation of the Si clathrates owing to the high heating rates of 800 °C h^{-1}. Even if the clathrates were crystallized during the heating process, they probably decomposed into Si and Na vapor upon heating to 800 °C.

Figure 4 shows schematic drawings of the mechanism we propose for the formation of double-helical Si microtubes.

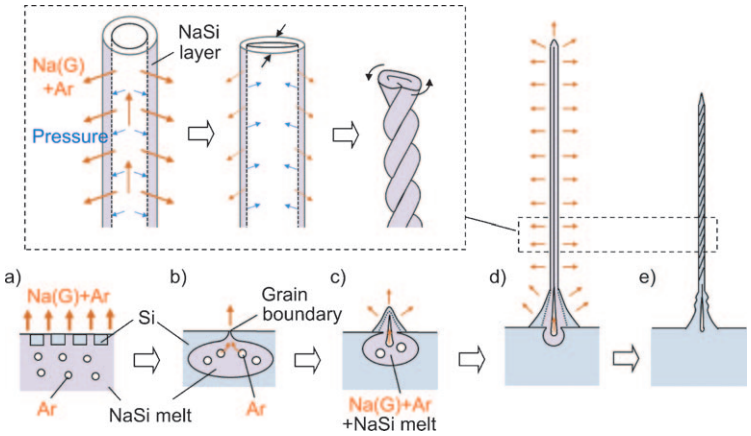

Figure 4. Proposed formation mechanism of double-helical Si microtubes. a) The disk surface is densely covered with Si grains, and b) some NaSi melts with Ar gas are trapped in the disk. c) The melts are exposed on the disk surface to the gas phase through the vent at the grain boundary, and protuberances are formed on the surface. d) The melt is pushed out and elongated to form a tube. e) The double-helical structure was formed by the evaporation of Na.

The starting NaSi disk is prepared by compaction of powdered NaSi in an Ar-filled glove box. The relative density of the disk is about 50–60 % of the theoretical density of NaSi. Many spaces filled with Ar gas are present among the grains in the compacted disk. Si grains crystallize during heating at a heating rate of 800 °C h^{-1}. Na is vaporized from the surface and inside of the disk through the spaces. At around a eutectic temperature of 750 °C, the disk surface is densely covered with Si grains (Figure 4a,b), and some NaSi melts with Ar gas are trapped in the disk (Figure 4b). If the melts with Ar gas are sealed with the Si grains (Figure 4b), the pressure of Ar gas slightly increases by heating from 750 to 800 °C. Na vapor is also included in Ar gas, but the vapor pressure of Na is 0.45 atm at 800 °C, and the equilibrium Na pressure is probably lower when the NaSi melt coexists.[22] The melts including Ar gas move toward the disk surface by dissolving Si at the grain boundary near the surface and by recrystallizing Si inside the disk.

Once the melts are exposed on the disk surface to the gas phase through the vent at the grain boundary, protuberances are formed on the surface (Figure 4c). Na immediately evaporates from the surface of the protuberances and a thin layer of fine Si grains covers the melt surface. If the gas pressure in the melt of a protuberance is still high enough, the melt is pushed out and elongated to form a tube (Figure 4d). However, the volume of the tube is rapidly decreased by evaporation of Na and crystallization of Si forming nanotwins. We speculate that this volume decrease is the driving force for the double-helical structure formation (Figure 4e). If the volume of the NaSi melt does not change so much from that of the NaSi crystal (29.4 cm^3 mol^{-1}), volume shrinkage from the melt to Si (12.1 cm^3 mol^{-1}) is about 40 %.

The formation of the double-helical microtubes may be realized by a very delicate balance between the inner pressure of the melt in the protuberance and the viscosity of the melt. If the viscosity is too high, the protuberance cannot be elongated, and if it is too low, the gas is easily released from the top of the protuberance. The formation of the melt including Ar gas inside the disk is necessary for the formation of the protuberances and Si double-helical tubes. Further experiments are needed to verify the hypothetical mechanism and to find a way to control the length and diameter of the tube, as well as to clarify the effect of additive elements such as boron or phosphorous against the morphology and properties. The effect of other gas species such as He and N_2 as well as Ar may also be interesting to study.

Besides the semiconducting characteristics, various properties such as visible light photoluminescence and thermoelectric performance reported for Si have been accomplished by fabrication of nanostructures.[23,24] Since the double-helical tubes consist of nanotwinned micrograins of Si and have many nanopores, some sort of confinement effects for the properties might be expected. Si whiskers and pipes prepared previously are mainly nano- to sub-micrometer-sized and single-crystalline. Nanotwins have been observed in Si thin films and nanorods, but the thickness and size are limited, and nanoholes are not included. The double-helical Si tubes with the peculiar microscale shape and morphology could be applied to some specific micro-order-sized applications, such as components of micromachines and screws. The sharp tips of the helical Si tubes could be fitted to microprobes and droppers. The nanosurface texture and nanoholes of the helical Si tubes may be suitable for application of absorbents, gas-sensors, and catalyst supports.

The characteristics of the double-helical Si microtubes have not been explored yet, but are expected to be clarified in the future.

Experimental Section

Si powder (High Purity Chemicals, 99.999 % purity, particle size < 75 μm) and Na (Nippon Soda, 99.95 % purity) were used for the preparation of NaSi. Si (0.30 g) and Na (0.25 g) (total 0.55 g) were weighed in an Ar gas-filled glove box (O_2 and H_2O < 1 ppm) at a Na:Si molar ratio of 1:1. This mixture of Si and Na was then placed in a boron nitride (BN) crucible (Showa Denko; 99.95 %; inside diameter 6 mm; depth 18 mm), which was then sealed in a stainless steel tube (inside diameter 10 mm; length 80 mm) with Ar. The sealed tube was heated at 700 °C for 24 h in an electric furnace. After cooling in the furnace, the tube was opened and the sample was taken out in the glove box. The obtained sample was powdered with an agate mortar and pestle, and confirmed to be NaSi (monoclinic, $a = 1.219$, $b = 0.655$, $c = 1.118$ nm, $\beta = 119.0°$, space group $C2/c$) by X-ray powder diffraction in Ar atmosphere (XRPD, $Cu_{K\alpha}$, Rigaku Rint-2200).[7]

NaSi powder (0.5 or 1.0 g) was compacted into a disk 15 mm in diameter and 2.5 mm thick or 25 mm in diameter and 2.0 mm thick. The disk was placed on a BN stage and sealed under Ar atmosphere in a stainless steel reactor (inside diameter 38 mm; depth 227 mm; Figure S3 in the Supporting Information). The bottom side of the container was heated at 800 °C, and a water-cooled jacket was attached to the other side. The heating rate of the bottom side was 800 °C h^{-1}. The sample was heated at 800 °C for 12 h. Na metal that evaporated from the sample was condensed on a cold trap and a cold

part of the reactor, and no Na was observed on the obtained sample on the BN stage. The sample was first washed with alcohol and then with distilled water. X-ray diffraction (XRD) data of the sample were collected using $Mo_{K\alpha}$ radiation with a graphite monochromator and an imaging plate on an X-ray diffractometer (Rigaku, R-AXIS RAPID-II). Photographs of the sample were taken with a digital camera, a digital optical microscope (KEYENCE, VHX-1000), a scanning electron microscope (Philips, ESEM XL-30, KEYENCE, VE-9800), and a transmission electron microscope (JEOL JEM-2000EX). The sample for TEM observation was prepared with an ion slicer (JEOL, EM-09100IS). Elemental analysis was carried out with an energy-dispersive X-ray (EDX) analyzer (EDAX, NEW XL-30) attached to the scanning electron microscope.

Received: December 24, 2009
Published online: April 12, 2010

Keywords: helical structures · microtubes · silicon · X-ray diffraction · Zintl phases

[1] S. Iijima, *Nature* **1991**, *354*, 56 – 58.
[2] N. Hamada, S. Sawada, A. Oshiyama, *Phys. Rev. Lett.* **1992**, *68*, 1579 – 1581.
[3] R. Saito, G. Dresselhaus, M. S. Dresselhaus, *Physical Properties of Carbon Nanotubes*, Imperial College Press, London, **1998**.
[4] S. Motojima, M. Kawaguchi, K. Nozaki, H. Iwanaga, *Appl. Phys. Lett.* **1990**, *56*, 321 – 323.
[5] D. Zhang, D. A. Alkhateeb, H. Han, H. Mahmood, D. N. McIlroy, M. G. Norton, *Nano Lett.* **2003**, *3*, 983 – 987.
[6] X. Y. Kong, Z. L. Wang, *Nano Lett.* **2003**, *3*, 1625 – 1631.
[7] R. S. Wagner, W. C. Ellis, *Appl. Phys. Lett.* **1964**, *4*, 89 – 90.
[8] A. T. Heitsch, D. D. Fanfair, H. Y. Tuan, B. A. Korgel, *J. Am. Chem. Soc.* **2008**, *130*, 5436 – 5437.
[9] J. D. Holmes, K. P. Johnston, R. C. Doty, B. A. Korgel, *Science* **2000**, *287*, 1471 – 1473.
[10] J. Q. Hu, Y. Bando, Z. W. Liu, J. H. Zhan, D. Golberg, T. Sekiguchi, *Angew. Chem.* **2004**, *116*, 65 – 68; *Angew. Chem. Int. Ed.* **2004**, *43*, 63 – 66.
[11] J. Sha, J. J. Niu, X. Y. Ma, J. Xu, X. B. Zhang, Q. Yang, D. Yang, *Adv. Mater.* **2002**, *14*, 1219 – 1221.
[12] J. Witte, H. G. Von Schnering, *Z. Anorg. Allg. Chem.* **1964**, *327*, 260 – 273.
[13] M. E. Straumanis, *J. Appl. Phys.* **1952**, *23*, 330 – 334.
[14] C. Cayron, Hertog M. Den, L. Latu-Romain, C. Mouchet, C. Secouard, J. L. Rouviere, E. Rouviere, J. P. Simonato, *J. Appl. Crystallogr.* **2009**, *42*, 242 – 252.
[15] Y. N. Xia, P. D. Yang, Y. G. Sun, Y. Y. Wu, B. Mayers, B. Gates, Y. D. Yin, F. Kim, Y. Q. Yan, *Adv. Mater.* **2003**, *15*, 353 – 389.
[16] J. Q. Hu, Y. Bando, Z. G. Liu, J. H. Zhan, D. Golberg, *Adv. Funct. Mater.* **2004**, *14*, 610 – 614.
[17] H. Morito, T. Yamada, T. Ikeda, H. Yamane, *J. Alloys Compd.* **2009**, *480*, 723 – 726.
[18] J. S. Kasper, P. Hagenmul, M. Pouchard, C. Cros, *Science* **1965**, *150*, 1713 – 1714.
[19] C. Cros, M. Pouchard, P. Hagenmuller, *J. Solid State Chem.* **1970**, *2*, 570 – 581.
[20] H. Horie, T. Kikudome, K. Teramura, S. Yamanaka, *J. Solid State Chem.* **2009**, *182*, 129 – 135.
[21] M. Beekman, G. S. Nolas, *Physica B* **2006**, *383*, 111 – 114.
[22] M. M. Makansi, C. H. Muendel, W. A. Selke, *J. Phys. Chem.* **1955**, *59*, 40 – 42.
[23] A. G. Cullis, L. T. Canham, *Nature* **1991**, *353*, 335 – 338.
[24] A. I. Hochbaum, R. K. Chen, R. D. Delgado, W. J. Liang, E. C. Garnett, M. Najarian, A. Majumdar, P. D. Yang, *Nature* **2008**, *451*, 163 – 167.

